ISSN 1070-3284, Russian Journal of Coordination Chemistry, 2018, Vol. 44, No. 5, pp. 340–346. © Pleiades Publishing, Ltd., 2018.

Syntheses, Structures, and Magnetic Properties of Two Mn(II) Coordination Polymers Based on 4-Fluorocinnamic Acid and 1,10-Phenanthroline[1]

H. X. Kang[a], Y. Q. Fu[b], F. Y. Ju[a], G. L. Li[a], X. L. Li[a], and G. Z. Liu[b, *]

[a] *School of Food and Drug, Luoyang Normal University, Luoyang Normal University, Henan, Luoyang, 471934 P.R. China*
[b] *College of Chemistry and Chemical Engineering, Luoyang Normal University, Henan, Luoyang, 471934 P.R. China*
**e-mail: gzliuly@126.com*

Received July 24, 2017

Abstract—Two Mn(II) coordination polymers, $\{[Mn_3(Pfca)_6(Phen)_2] \cdot 2DMF\}_n$ (**I**) and $[Mn(Pfca)_2(Phen)(H_2O)]_n$ (**II**) (HPfca = 4-fluorocinnamic acid, Phen = 1,10-phenanthroline), were synthesized and characterized by elemental analysis, IR spectroscopy, thermogravimetric analysis, and single-crystal X-ray diffraction (CIF files CCDC nos. 967513 (**I**), 1542972 (**II**)). Complex **I** crystallizes in the triclinic crystal system, space group $P\bar{1}$ with a = 11.0821(11), b = 12.2632(12), c = 15.0288(15) Å, α = 87.3760(10)°, β = 88.4610(10)°, γ = 81.2220(10)°, V = 2016.0(3) Å^3, ρ_c = 1.369 g/cm^3, M_r = 1662.25, Z = 1, $F(000)$ = 853, μ = 0.543 mm^{-1}, the final R = 0.0592 and wR = 0.1681 for 15498 observed reflections with $I > 2\sigma(I)$. Complex **II** is of monoclinic system, space group $P2_1/c$ with a = 18.0539(19), b = 8.5806(9), c = 18.758(2) Å, β = 116.5700(10)°, V = 2599.0(5) Å^3, ρ_c = 1.491 g/cm^3, M_r = 583.44, Z = 4, $F(000)$ = 1196, μ = 0.567 mm^{-1}, the final R = 0.0337 and wR = 0.0853 for 18139 observed reflections with $I > 2\sigma(I)$. Complex **I** features linear Mn(II)-trinuclear units, which form 1D chain structure through F···F weak interactions, and complex **II** is 1D polymeric Mn(II)-chains. Antiferromagnetic coupling interactions exist within Mn(II)-carboxylate trinuclear in **I** (J = –0.40 cm^{-1}) and Mn(II)-carboxylate chain in **II** (J = –0.45 cm^{-1}).

Keywords: 4-fluorocinnamic acid, Mn(II) coordination polymers, single-crystal X-ray diffraction, magnetic properties

DOI: 10.1134/S1070328418050020

INTRODUCTION

In recent years, the coordination complexes magnetism has been achieved much success in synthesizing a large of new magnetic materials, which provides an effective way to design magnetic systems when magnetic metal ions are assembled into coordination complexes by employing suitable ligands [1, 2]. The ligands with carboxyl groups [3–6], azaheterocyclic structure [7–9] and short bridging groups (hydroxyl, oxygen, cyano, and azido) are good candidates for constructing the novel magnetic materials [10–18]. The researches show that most of them display antiferromagnetic or ferrimagnetic interactions. For the reason that the value of the exchange coupling between metal ions through bridging carboxylate (J) is affected by the bridging mode of the carboxylate and the type of M–O–C–O–M pathway involved, the synthesis of carboxylato-bridged transition metal complexes appeals to many researchers [5, 19, 20].

Cinnamic acid and its derivates have plentiful coordinated modes, and the mononuclear, dinuclear, trinuclear, 1D, 2D, 3D coordination polymers have been synthesized and reported [21–28]. Especially the carboxylate group of cinnamic acid conjugates with benzene ring through C=C double bond and may implement single-crystal to single-crystal (SC–SC) structural transformation of complex by photochemical [2 + 2] cycloaddition reaction.

However the coordination polymers based on the 4-fluorocinnamic acid (Pfca) ligand are seldom reported. Compared to the cinnamic acid, the F$^-$ substituted cinnamic acid can form F···F and F···H weak interactions, which can reinforce the crystal packing and construct more flexible structures. The Co(II), Cu(II), Ni(II) coordination polymers with Pfca ligand were obtained in our previous work [22, 23]. In the further research we obtained two new Mn(II) coordination complexes by the mixed-ligand strategy in the presence of Pfca and 1,10-phenanthroline (Phen). Complex $\{[Mn_3(Pfca)_6(Phen)_2] \cdot 2DMF\}_n$ (**I**) features

[1] The article is published in the original.

linear Mn(II)-trinuclear units, which form 1D chain structure through interchain F···F weak interactions. Complex $[Mn(Pfca)_2(Phen)(H_2O)]_n$ (**II**) is 1D polymeric Mn(II)-chains formed by the *syn-syn* bridging coordination of Pfca carboxyl groups. The magnetic susceptibility measurements indicate the occurrence of classic antiferromagnetic coupling interactions within Mn(II)-trinuclear units in **I** and Mn(II)-carboxylate 1D chain in **II**.

EXPERIMENTAL

Materials and physical measurements. All reagents were of analytical grade and used as purchased without further purification. Elemental analyses for carbon, hydrogen and nitrogen were performed with a Flash 2000 organic elemental analyzer. The FT-IR spectra were recorded on powdered samples using a NICOLET 6700 FT-IR spectrometer in the 4000–600 cm^{-1} range. Powder X-ray diffraction (PXRD) patterns were recorded with a Bruker D8 ADVANCE X-ray diffractometer at the room temperature. Thermogravimetric analysis (TGA) was performed on a STA449C integration thermal analyzer in flowing N_2 with a heating rate of 10°C/min.

Synthesis of complex I. A methanol solution (3 mL) of $MnCl_2 \cdot 4H_2O$ (0.2 mmol, 0.040 g) was mixed with a methanol (5 mL) solution of (E)-3-(3-fluoro-phenyl)-acrylic acid (0.6 mmol, 0.099 g). Triethylamine (0.6 mmol, 0.060 g) was added drop-wise to this mixture to bring the pH of the solution to about 7 with constantly stirring for 30 min. Then Phen (0.3 mmol, 0.059 g) was added to this mixture with constantly stirring by adding about 2 mL DMF. The mixture was refluxed for 2 h. The result solution was then filtered and left at room temperature. Yellow rectangular shaped single crystals suitable for X-ray diffraction were obtained by slow evaporation for about 20 days allowed to dry in air. The yield is 75% (based on Mn).

For $C_{84}H_{66}N_6O_{14}F_6Mn_3$			
Anal. calcd., %	C, 60.64	H, 3.97	N, 5.05
Found, %	C, 60.76	H, 3.83	N, 4.96

Synthesis of complex II. The synthesis of the complex **II** was in a same procedure to that of complex **I** besides the shorter evaporation time than **I** (about 7 days). Yellow rectangular shaped crystals were obtained with 52% yield (based on Mn).

For $C_{30}H_{22}N_2O_5F_2Mn$			
Anal. calcd., %	C, 61.70	H, 3.77	N, 4.80
Found, %	C, 61.32	H, 3.86	N, 4.87

X-ray structure determination. Diffraction data were collected on a Bruker SMART APEX CCD diffractometer equipped with a graphite-monochromated MoK_α (λ = 0.71073 Å) radiation by using a φ–ω scan mode at room temperature. Absorption corrections were based on symmetry equivalent reflections using the SADABS program [29]. The structures were solved by direct methods and refined by full-matrix least-squares on F^2. All calculations were performed using the SHELXTL-97 program package [30]. All non-hydrogen atoms in complexes **I** and **II** were refined with anisotropic thermal parameters. The hydrogen atoms were placed in the calculated positions and refined isotropically with a riding model except for those bound to water molecules and hydroxyl groups, which were initially located in a difference Fourier map and included in the final refinement by use of geometrical restraints. The crystal data as well as the details of data collection and refinements for **I** and **II** are listed in Table 1. Selected lengths and angles parameters are given in Table 2.

Supplementary materials for two compounds have been deposited with Cambridge Crystallographic Data Centre (CCDC nos. 967513 (**I**), 1542972 (**II**); deposit@ccdc.cam.ac.uk or http://www.ccdc.cam.ac.uk/data-request/cif).

RESULTS AND DISCUSSION

The asymmetric unit of complex **I** contains one and a half Mn(II) atoms located at the crystallographic center, one Phen, three Pfac ligands, one lattice DMF molecule (Fig. 1a). The structure displays a linear trinuclear Mn(II) unit (Fig. 1b). All the Mn^{2+} ions are six-coordinated with a distorted octahedral geometry. The coordination sphere of Mn(1) is coordinated by six O atoms from six different Pfca anions (Mn–O 2.144(3)–2.192(3) Å). The coordination sphere of Mn(2) is defined by four O atoms from three different Pfca anions (Mn–O 2.094(3)–2.204(3) Å) and two N atoms from one Phen molecule (Mn–N 2.250(3)–2.287(3) Å).

The linear trinuclear unit is completely assembled in such a way that the central $Mn(1)O_6$ octahedron is connected to two $Mn(2)O_4N_2$ octahedra at two ends by one bidentate Pfca anion with a μ_3-η^1:η^2 bridging coordination mode and two tridentate Pfca anions with a μ_2-η^1:η^1 bridging coordination mode. The distance between the two adjacent Mn^{2+} ions is 3.5587(6) Å within the trinuclear unit.

It is clear that halogen–halogen contacts are characterized by the fact that the interhalogen distance is less than the sum of van der Waals radii (r_{vdW}) of the corresponding halogen atoms. The r_{vdW} of the fluoro atom is 1.47 Å, and the shortest F···F distance is 2.6566(66) Å in complex **I** (Fig. 1c). So the F···F interactions exist in this complex. Furthermore, the trinuclear Mn(II) units are connected to form a 1D chain along the *b* direction through the F···F interactions. The 1D chains are cohered together by weak

Table 1. Crystallographic and structure refinement data for complexes **I** and **II**

Parameter	Value	
	I	**II**
Temperature, K	296(2) K	296(2) K
Crystal system	Triclinic	Monoclinic
Space group	$P\bar{1}$	$P2_1/n$
a, Å	11.0821(11)	18.0539(19)
b, Å	12.2632(12)	8.5806(9)
c, Å	15.0288(15)	18.758(2)
α, deg	87.3760(10)	90
β, deg	88.4610(10)	116.5700(10)
γ, deg	81.2220(10)	90
Volume, Å^3	2016.0(3)	2599.0(5)
Crystal size, mm	0.35 × 0.27 × 0.10	0.33 × 0.25 × 0.17
Z	1	4
ρ_{calcd}, g cm^{-3}	1.369	1.491
μ, mm^{-1}	0.541	0.567
F(000)	853	1196
θ Range, deg	2.31–25.50	2.43–25.50
Reflections collected	15498	18139
Independent reflections (R_{int})	7455 (0.0266)	4833 (0.0275)
Parameters	513	361
Goodness-of-fit	1.004	1.108
Final R indices ($I > 2\sigma(I)$)	$R_1 = 0.0592$, $wR_2 = 0.1681$	$R_1 = 0.0337$, $wR_2 = 0.0853$
R indices (all data)	$R_1 = 0.0879$, $wR_2 = 0.1932$	$R_1 = 0.0458$, $wR_2 = 0.0938$
Largest diff. peak and hole, e Å^{-3}	0.790 and –0.684	0.479 and –0.259

van der Waals force to form a 3D supermecular network (Fig. 1d).

In complex **II**, the asymmetric unit contains one crystallographic Mn(II) atom, one Phen, two Pfca anions, one water molecule (Fig. 2a). The Mn(II) center is octahedrally coordinated by three carboxylate O atoms from three different Pfac ligands, one water O atom and two Phen N atoms. The N(1), N(2), O(2*A*), O(3) are in the equatorial plane, leaving two apical positions occupied by O(5) and O(1) atoms. The Mn–O bond lengths are between 2.141(1) and 2.243(1) Å, and two Mn–N bond lengths are 2.291(2) and 2.334(2) Å. The adjacent Mn^{2+} ions are connected by Pfca anions adopting a μ_2-η^1:η^1 bridging coordination mode to form a 1D linear chain along y direction with the Mn···Mn distance of 5.2640(6) Å (Fig. 2b). The further assembly among the 1D chains to form its final 3D supermolecular structure is completed through weak van der Waals force.

The both complexes are further characterized by the IR spectra, which were consistent with their structures as determined by single-crystal X-ray diffraction. The strong absorptions at 1640, 1388 cm^{-1} for **I** and 1646, 1402 cm^{-1} for **II** are attributed to the asymmetric stretching vibration $\nu_{as}(COO^-)$ and the symmetric stretching vibration $\nu_s(COO^-)$, respectively. The strong absorptions at 1415 cm^{-1} for **I** and 1420 cm^{-1} for **II** can be ascribed to C=N stretching modes of Phen. The absorptions at 1268 cm^{-1} for **I** and 1275 cm^{-1} for **II** are attributed to C–F characteristic absorptions.

PXRD of complexes **I** and **II** have been studied at room temperature, which are in good agreement with the patterns simulated from the respective single-crystal data, implying the good phase purity of two complexes.[2]

The experiments of TGA of complexes **I** and **II** were performed on the crystalline samples from 25 to 850°C at a heating rate of 5°C min^{-1} under nitrogen atmosphere (Fig. 3). There are two steps in the decomposition process for complex **I**. The first weight loss of 8.3% from 110 to 150°C corresponds approxi-

[2]Additional experimental data can be requested from authors.

Table 2. Selected bond lengths (Å) and angles (deg) for complexes **I** and **II***

Bond	*d*, Å	Bond	*d*, Å
		I	
Mn(1)–O(3)	2.144(3)	Mn(1)–O(3)$^{\#1}$	2.144(3)
Mn(1)–O(5)$^{\#1}$	2.186(3)	Mn(1)–O(1)	2.192(3)
Mn(2)–O(4)	2.094(3)	Mn(2)–O(2)	2.096(3)
Mn(2)–N(2)	2.250(3)	Mn(2)–N(1)	2.287(3)
Mn(1)–O(5)	2.186(3)	Mn(1)–O(1)$^{\#1}$	2.192(3)
Mn(2)–O(5)	2.204(3)	Mn(2)–O(6)	2.370(3)
		II	
Mn(1)–O(3)	2.1408(14)	Mn(1)–O(2)$^{\#1}$	2.1606(14)
Mn(1)–O(5)	2.2429(14)	Mn(1)–N(2)	2.291(2)
Mn(1)–O(1)	2.1755(14)	Mn(1)–N(1)	2.334(2)
Angle	*d*, deg	Angle	*d*, deg
		I	
O(3)Mn(1)O(3)$^{\#1}$	180.0(2)	O(3)Mn(1)O(5)	91.22(11)
O(3)Mn(1)O(5)$^{\#1}$	88.78(11)	O(3)$^{\#1}$Mn(1)O(5)$^{\#1}$	91.22(11)
O(3)Mn(1)O(1)	89.89(12)	O(3)$^{\#1}$Mn(1)O(1)	90.11(12)
O(5)$^{\#1}$Mn(1)O(1)	89.50(11)	O(3)Mn(1)O(1)$^{\#1}$	90.11(12)
O(5)Mn(1)O(1)$^{\#1}$	89.50(11)	O(5)$^{\#1}$Mn(1)O(1)$^{\#1}$	90.50(11)
O(4)Mn(2)O(2)	95.83(13)	O(4)Mn(2)O(5)	104.50(12)
O(4)Mn(2)N(2)	91.57(12)	O(2)Mn(2)N(2)	108.89(12)
O(4)Mn(2)N(1)	164.04(12)	O(2)Mn(2)N(1)	87.43(13)
O(5)Mn(2)N(1)	90.60(12)	N(2)Mn(2)N(1)	72.63(12)
O(2)Mn(2)O(6)	152.48(12)	O(5)Mn(2)O(6)	56.90(10)
O(3)$^{\#1}$Mn(1)O(5)	88.78(11)	O(2)Mn(2)O(5)	96.47(11)
O(5)Mn(1)O(5)$^{\#1}$	180.0(2)	O(5)Mn(2)N(2)	148.46(11)
O(5)Mn(1)O(1)	90.50(11)	O(5)Mn(2)N(1)	90.60(12)
O(3)$^{\#1}$Mn(1)O(1)$^{\#}$1	89.89(12)	O(4)Mn(2)O(6)	97.65(12)
O(1)Mn(1)O(1)$^{\#1}$	180.00(16)	N(2)Mn(2)O(6)	94.64(11)
N(1)Mn(2)O(6)	86.16(12)		
		II	
O(3)Mn(1)O(2)$^{\#1}$	107.96(6)	O(3)Mn(1)O(1)	89.11(5)
O(3)Mn(1)O(5)	85.97(5)	O(2)$^{\#1}$Mn(1)O(5)	86.44(5)
O(3)Mn(1)N(2)	157.72(6)	O(2)$^{\#1}$Mn(1)N(2)	93.37(6)
O(5)Mn(1)N(2)	89.09(6)	O(5)Mn(1)N(2)	89.09(6)
O(2)$^{\#1}$Mn(1)N(1)	165.02(6)	O(1)Mn(1)N(1)	98.20(6)
O(2)$^{\#1}$Mn(1)O(1)	84.74(5)	O(3)Mn(1)N(1)	86.83(6)
O(1)Mn(1)O(5)	168.06(6)	O(5)Mn(1)N(1)	92.39(6)
O(1)Mn(1)N(2)	99.44(6)	N(2)Mn(1)N(1)	71.67(6)

* Symmetry codes for complexes: $^{\#1}$ $-x$, $-y+1$, $-z+1$ (**I**); $^{\#1}$ $-x+3/2$, $y-1/2$, $-z+1/2$ (**II**).

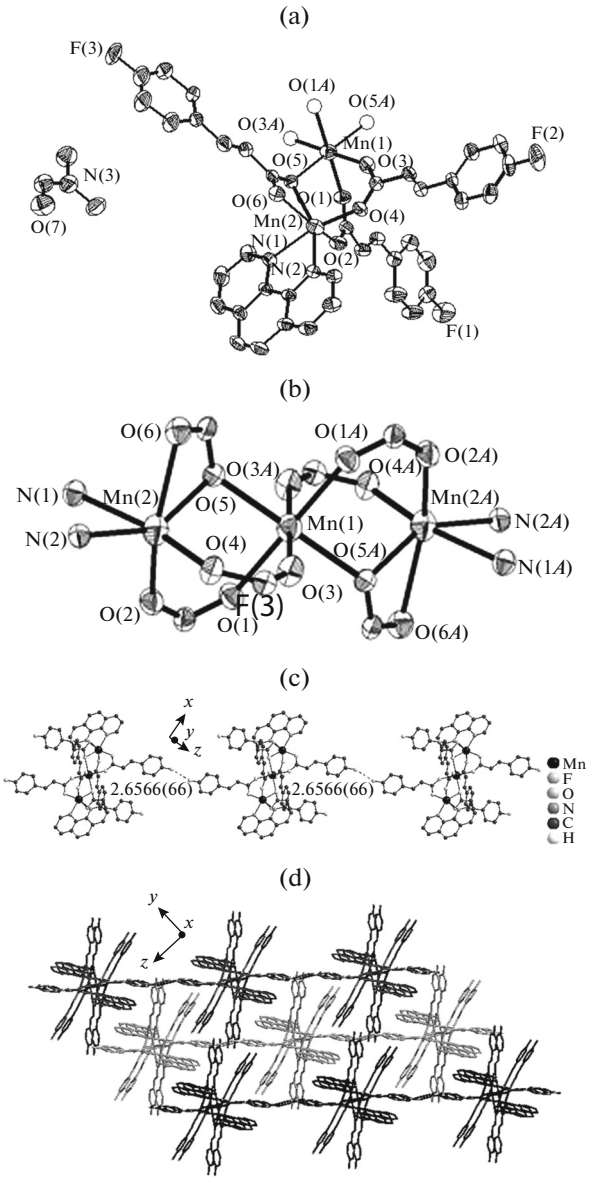

Fig. 1. View of the asymmetric unit showing the coordination environment of Mn^{2+} cation in complex **I** (symmetry codes: $A = -x + 2, -y, -z$) (a); view of the trinuclear unit (b); details of F···F interactions between adjacent trinuclear units (c); view of 3D supermolecular structure (d).

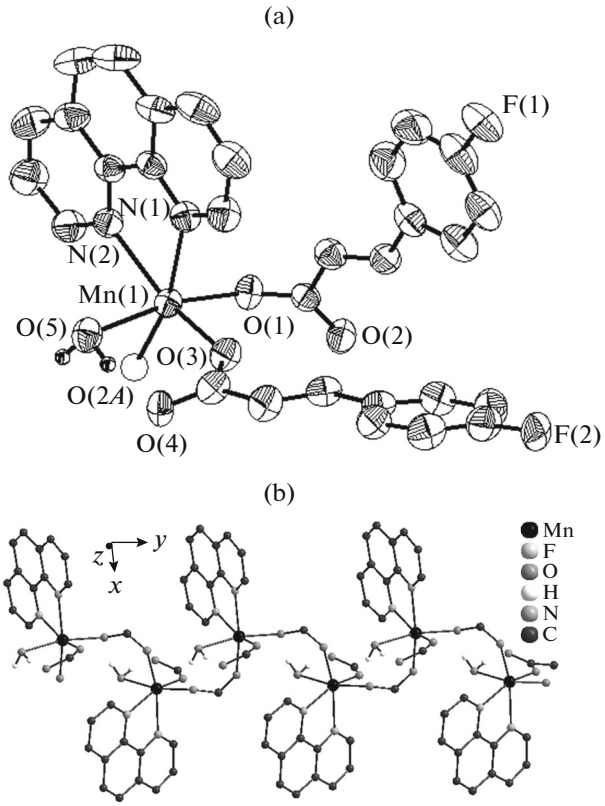

Fig. 2. View of the asymmetric unit showing the coordination environment of Mn^{2+}cation in complex **II** (symmetry codes: $A = -x + 3/2, y - 1/2, -z + 1/2$; $B = -x + 3/2, y + 1/2, -z + 1/2$) (a); view of 1D polymeric chain (Pfca ligands omitted for clarity) (b).

mately to release the two lattice DMF molecules per formula unit (calcd. 8.8%). The second mass weight loss takes place over 270°C, being attributed to the decomposition of organic components. The final residue cannot be specifically identified and may be a mixture. For complex **II**, a 3.12% weight loss in the region of 110–165°C corresponds to the loss of one coordinated water molecule per formula unit (calcd. 3.1%). Over 245°C, the residue starts to decompose and does not stop until the heating end at 850°C.

The magnetic properties of Mn(II) complexes have attracted much attention due to the characteristics of intramolecular electron transfer and magnetic exchange. So the magnetic susceptibilities (χ_M) of **I** and **II** were investigated in the 2.0–300.0 K range at 2000 Oe applied field. The results are shown as $\chi_M T$ and χ_M versus T plots in Fig. 4.

Complex **I** is a symmetrical linear Mn(II) trinuclear and the magnetic interactions can be considered to occur between the adjacent metal ions within the trinuclear unit. The reason to ignore the magnetic interactions between the adjacent trinuclear units is that the center-to-center distances between the two trinuclear units are larger than 11 Å. The $\chi_M T$ value is 12.12 $cm^3\ mol^{-1}$ K at 300 K, close to the value of 13.125 $cm^3\ mol^{-1}$ K, which corresponds to three uncoupled Mn^{2+} ions. When the temperature decreases, the $\chi_M T$ values fall until reaching 5.97 $cm^3\ mol^{-1}$ K at 2 K, which are higher than the expected value of 4.375 $cm^3\ mol^{-1}$ K for a spin ground state $S_T = 5/2$ and $g = 2$, indicative of an antiferromagnetic coupling. The magnetic susceptibility obeys the Curie–Weiss law [$\chi_M^{-1} = (T - \theta)/C$] above 8 K with a Weiss constant θ of −3.07 K and a Curie constant C of 13.03 $cm^3\ mol^{-1}$ K. The negative θ value further sug-

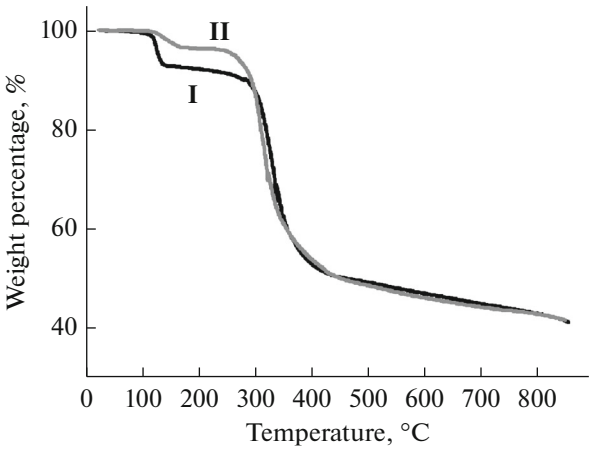

Fig. 3. TGA curve of complexes **I** and **II**.

gests the antiferromagnetic coupling within the trinuclear unit.

In order to evaluate the magnetic interactions quantitatively, the experimental data for **I** were modeled using Eqs. (1) and (2) with $S = 5/2$ [31–33]. The least-squares analysis of magnetic susceptibilities data led to $J = 0.39$ cm^{-1}, $g = 2.10$, $R = 8.93 \times 10^{-4}$.

$$\chi_M = \frac{2Ng^2\beta^2}{KT}\frac{A}{B}, \quad (1)$$

$$A = 14x^{44} + 5x^{40} + 31x^{36} + 14x^{34} + 5x^{32} + x^{30} + 105x^{26} + 5x^{22} + 19x^{20} + 30x^{18} + 69x^{16} + 91x^{14} + 30x^{12} + 55x^{8} + 91x^{4} + 140,$$

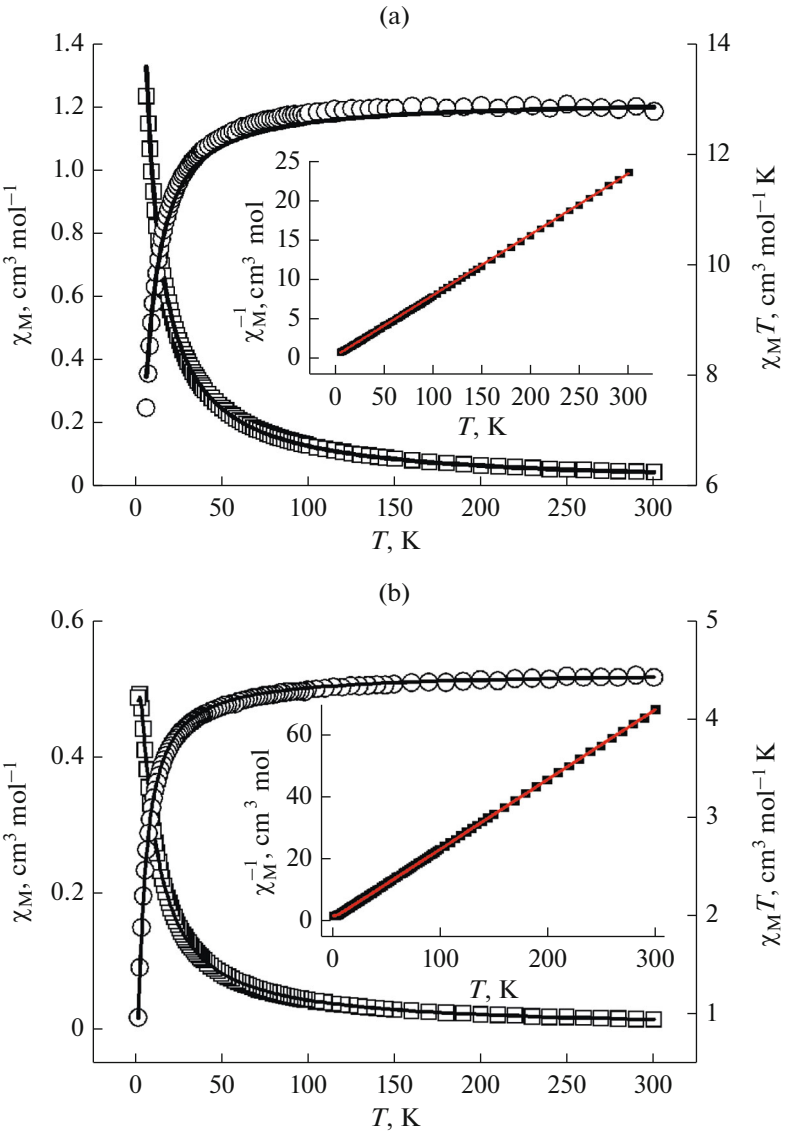

Fig. 4. Plot of the $\chi_M T$ (○) and χ_M (□) versus T in complex **I** (a) and **II** (b). Open points are the experimental data, and the solid line represents the best-fit curve. The field strength used was $H = 2000$ Oe. Inset: χ_M^{-1} versus T.

$$B = 7x^{44} + 5x^{40} + 12x^{36} + 7x^{34} + 6x^{32} + 3x^{30} + 35x^{26} + 5x^{22} + 12x^{20} + 9x^{18} + 18x^{16} + 13x^{14} + 9x^{12} + 11x^{8} + 13x^{4} + 15,$$

$$x = \exp(-J/KT)$$

$$\chi'_{M} = \frac{\chi_{M}}{1 - (7.74zJ'/g^{2})\chi_{M}}. \quad (2)$$

For **II** the smallest Mn···Mn separation is 5.2640(6) Å in the intrachain, which is shorter than that (8.6517 Å) between chains. So, the possible magnetic superexchange pathway is mainly inside the 1D chain. The experiment shows that the $\chi_M T$ value at 300 K in 2 of 4.40 $cm^3\ mol^{-1}$ K is close to spin-only value (4.38 $cm^3\ mol^{-1}$ K, $S = 5/2$) expected for an isolated high-spin Mn^{2+} ion. As the temperature is lowered to 2 K the $\chi_M T$ values decrease, reaching a minimum of 0.96 $cm^3\ mol^{-1}$ K. This behavior suggests the existence of weak antiferromagnetic exchange behavior between the Mn^{2+} cations. The temperature dependence of the reciprocal susceptibilities ($1/\chi_M$) obeys the Curie–Weiss law with $\theta = -4.66$ K, $C = 4.17\ cm^3\ mol^{-1}$ K above 4 K. The intramolecular antiferromagnetic coupling is confirmed by the negative θ value. With the purpose of quantitatively evaluating the magnetic interactions, for similar 1D chain Mn(II) complexes, the experimental data for **II** were modeled using Eq. (3) with $S = 5/2$ [34]. The least-squares analysis of magnetic susceptibilities data led to $J = -0.45\ cm^{-1}$, $g = 2.02$, $R = 4.78 \times 10^{-5}$. The J value reveals further that weak antiferromagnetic interactions between the adjacent Mn^{2+} ions mediating through the *syn-syn* carboxylate bridging mode.

$$\chi_{chain} = \left[Ng^2\beta^2 S(S+1)/3kT \right] \times \left[(1+\mu)/(1-\mu) \right]. \quad (3)$$

ACKNOWLEDGMENTS

This work was supported by the National Natural Science Foundation of China (nos. 21571093 and 21271098), the Program for Science and Technology Innovation Talents in Universities of Henan Province (no. 14HASTIT017), the Project of Science and Technology in Henan Province (no. 172102310441), the Program for Innovative Research Team (in Science and Technology) in University of Henan Province (no. 14IRTSTHN008), and the Foundation of Education Committee of Henan Province (no. 142300410301).

REFERENCES

1. Kurmoo, M., *Chem. Soc. Rev.*, 2009, vol. 38, p. 1353.
2. Weng, D.F., Wang, Z.M., Gao, S., et al., *Chem. Soc. Rev.*, 2011, vol. 40, p. 3157.
3. Li, G.L., Yin, W.D., Liu, G.Z., et al., *J. Solid State Chem.*, 2014, vol. 220, p. 1.
4. Beobide, G., Wang, W.G., Castillo, O., et al., *Inorg. Chem.*, 2008, vol. 47, p. 5267.
5. Jin, X., Zhou, P., Zheng, C.Y., et al., *J. Solid State Chem.*, 2015, vol. 225, p. 41.
6. Niu, C.Y., Zheng, X.F., Wan, X.S., et al., *Cryst. Growth. Des.*, 2011, vol. 11, p. 2874.
7. Hu, H.C., Kang, X.M., Cao, C.S., et al., *Chem. Commun.*, 2015, vol. 51, p. 10850.
8. Sengupta, O. and Mukeherjee, P.S., *Inorg. Chem.*, 2010, vol. 49, p. 8583.
9. Li, J.R., Yu, Q., and Sanudo, E.C., *Chem. Mater.*, 2008, vol. 20, p. 1218.
10. Ouellette, W., Yu, M.H., Charles, J., et al., *Angew. Chem. Int. Ed.*, 2006, vol. 45, p. 3497.
11. Aromí, G., Stoeckli-Evans, H., Teat, S.J., et al., *J. Mater. Chem.*, 2006, vol. 16, p. 2635.
12. Singh, S. and Roesky, H.W., *Dalton Trans.*, 2007, vol. 14, p. 1360.
13. Chelebaeva, E., Larionnva, J., and Guari, Y., *Inorg. Chem.*, 2009, vol. 48, p. 5983.
14. Herchel, R., Travnicek, Z., Zboril, R., et al., *Inorg. Chim. Acta*, 2011, vol. 365, p. 458.
15. Ghosh, A.K., Ghoshal, D., Zangrando, E., et al., *Inorg. Chem.*, 2005, vol. 44, p. 1786.
16. Kurmoo, M.J. and Kepert, C., *New J. Chem.*, 1998, vol. 22, p. 1515.
17. Erkarslan, U., Oylumluoglu, G., Coban, M.B., et al., *Inorg. Chim. Acta*, 2016, vol. 445, p. 57.
18. Lian, Q.Y., Hu, H.N., Li, C.H., et al., *Chin. J. Struct. Chem.*, 2017, vol. 36, p. 273.
19. Maji, T.K., Sain, S., Mostafa, G., et al., *Inorg. Chem.*, 2003, vol. 42, p. 709.
20. Delgado, F.S., Sanchiz, J., Ruiz-Perez, C., et al., *Inorg. Chem.*, 2003, vol. 42, p. 5938.
21. Liu, G.L. and Liu, C.M., *J. Solid State Chem.*, 2011, vol. 184, p. 481.
22. Kang, H.X., Duan, Y.H., Yang, R.J., et al., *Z. Kristallogr. New. Cryst. Struct.*, 2015, vol. 230, p. 280.
23. Kang, H.X., Fu, Y.Q., Xin, L.Y., et al., *Chin. J. Struct. Chem.*, 2016, vol. 35, p. 286.
24. Zhou, X.J., Zhou, K.N., Wang, Z.Q., et al., *Chin. J. Inorg. Chem.*, 2013, vol. 29, p. 1870.
25. Fang, Y., Wang, L., Ni, L., et al., *Chin. J. Inorg. Chem.*, 2013, vol. 29, p. 1551.
26. Zhang, C.Y., Fu, J.D., and Wen, Y.H., *Chin. J. Inorg. Chem.*, 2011, vol. 27, p. 2308.
27. Li, H. and Hu, C.W., *J. Mol. Struct.*, 2005, vol. 743, p. 97.
28. Li, H. and Hu, C.W., *J. Solid State Chem.*, 2004, vol. 177, p. 4501.
29. Sheldrick, G.M., *A Program for the Siemens Area Detector Absorption Correction*, Göttingen: Univ. of Göttingen, 1997.
30. Sheldrick, G.M., *SHELXS-97, Program for the Solution of Crystal Structure*, Göttingen: Univ. of Göttingen, 1997.
31. Liu, B., Xu, L., Guo, G.C., et al., *J. Mol. Struct.*, 2006, vol. 825, p. 79.
32. Sinn, E., *Chem. Rev.*, 1970, vol. 5, p. 313.
33. Brown, D.B., Wasson, J.R., Hall, J.W., et al., *Inorg. Chem.*, 1977, vol. 16, p. 2526.
34. Fisher, M.E., *Am. J. Phys.*, 1964, vol. 32, p. 343.